THE EUROPEAN
PHYSICAL JOURNAL C

CrossMark

Regular Article - Theoretical Physics

Radiative neutrino mass model with degenerate right-handed neutrinos

Shoichi Kashiwase[a], **Daijiro Suematsu**[b]

Institute for Theoretical Physics, Kanazawa University, Kanazawa 920-1192, Japan

Abstract The radiative neutrino mass model can relate neutrino masses and dark matter at a TeV scale. If we apply this model to thermal leptogenesis, we need to consider resonant leptogenesis at that scale. It requires both finely degenerate masses for the right-handed neutrinos and a tiny neutrino Yukawa coupling. We propose an extension of the model with a $U(1)$ gauge symmetry, in which these conditions are shown to be simultaneously realized through a TeV scale symmetry breaking. Moreover, this extension can bring about a small quartic scalar coupling between the Higgs doublet scalar and an inert doublet scalar which characterizes the radiative neutrino mass generation. It also is the origin of the Z_2 symmetry which guarantees the stability of dark matter. Several assumptions which are independently supposed in the original model are closely connected through this extension.

1 Introduction

ATLAS and CMS groups in the LHC experiment have reported the discovery of the Higgs-like particle [1,2]. All the standard model contents seem to have been found by now. However, the standard model has serious problems from experimental and observational view points. Although the existence of neutrino masses and dark matter has been confirmed through various experiments and observations [3–14], it cannot be explained in the standard model. The standard model cannot give a framework for the generation of baryon number asymmetry in the Universe, either [15–17]. These facts now cause serious tension between the standard model and Nature so that they motivate us to consider its extension.

The radiative neutrino mass model proposed in [18] is a simple and interesting extension of the standard model which could be an explanation. In several previous articles [19–36], we have studied these problems in this model and its exten-

sions. They suggest that these problems could be explained in a consistent way, simultaneously. Unfortunately, however, we could not justify several assumptions and the parameter tuning adopted in these explanations. For example, if we consider thermal leptogenesis in this model, both finely degenerate right-handed neutrino masses and a small Yukawa coupling for the lightest right-handed neutrino are required in order to make possible sufficient generation of lepton number asymmetry through the out-of-equilibrium decay of the lightest right-handed neutrino. In this work, we have just assumed them independently in a way consistent with other phenomenological issues.

In this paper, we consider an extension of the model which makes it possible to realize these required conditions simultaneously in the evolution of the Universe. We suppose a new symmetry breaking at a scale of $O(1)$ TeV for this purpose. After this symmetry breaking, a small mass difference is induced between two lighter right-handed neutrinos, although they have an equal mass originally. At the same time, a Yukawa coupling of the lightest right-handed neutrino becomes much smaller than that of the heavier one. To realize this scenario, we introduce a low energy $U(1)$ gauge symmetry to the model. We show that (i) both the almost degenerate right-handed neutrino masses and a tiny neutrino Yukawa coupling, which are indispensable for TeV scale resonant leptogenesis [37–40], are brought about after the breaking of this symmetry. Moreover, we find that this extension can also explain important key features required in the original Ma model, that is, (ii) a small quartic coupling between the Higgs doublet scalar and an inert doublet scalar which plays a crucial role in the neutrino mass generation, and (iii) the origin of the Z_2 symmetry which guarantees the stability of dark matter.

The remaining part of this paper is organized as follows. After introducing an extended model in the next section, we discuss features in the scalar sector and also the right-handed neutrino mass degeneracy. Baryon number asymmetry generated through the thermal leptogenesis is studied

[a] e-mail: shoichi@hep.s.kanazawa-u.ac.jp

[b] e-mail: suematsu@hep.s.kanazawa-u.ac.jp

taking account of these. In Sect. 3, we study the dark matter relic abundance and other cosmological aspects of the model. Finally, in Sect. 4 we give a brief summary of the main results of the paper.

2 An extended model

2.1 $U(1)$ gauge symmetry at a TeV scale

The original Ma model is a simple extension of the standard model which can relate neutrino masses and dark matter [18]. In this model, only an inert doublet scalar η and right-handed neutrinos N_i are added to the standard model. Although ingredients of the standard model are assigned an even parity of the imposed Z_2 symmetry, new fields are assumed to have odd parity. This feature forbids tree-level neutrino mass generation and guarantees the stability of dark matter.

We extend this model with a $U(1)_X$ gauge symmetry, a singlet scalar S, and also additional right-handed neutrinos $\tilde{N}_i$ whose number is equal to the one of N_i. The $U(1)_X$ charge is assigned each new ingredient as $Q_X(S) = 2$, $Q_X(\eta) = -1$, $Q_X(N_i) = 1$, and $Q_X(\tilde{N}_i) = -1$. Normalization for the $U(1)_X$ charge and coupling is fixed through a covariant derivative, which is defined as $D_\mu = \partial_\mu - ig\frac{\tau^a}{2}W_\mu^a - ig_Y\frac{Y}{2}B_\mu - ig_X\frac{Q_X}{2}X_\mu$. Since the standard model fields are assumed to have no charge for this $U(1)_X$, it is obvious that the $U(1)_X$ is anomaly free. If this symmetry is assumed to break down due to a vacuum expectation value $\langle S \rangle$, the model has a remnant exact symmetry Z_2 after this breaking. Since only η, N_i, and $\tilde{N}_i$ have odd parity, the lightest one of them is stable and can be dark matter. We assume that dark matter is the lightest neutral component of η in this study.

The relevant part of the Lagrangian for these new ingredients of the model is summarized as

$$
\begin{aligned}
-\mathcal{L}_N = {} & h_{\alpha i}\bar{N}_i\eta^\dagger\ell_\alpha + f_{\alpha i}\frac{S^\dagger}{M_*}\bar{\tilde{N}}_i\eta^\dagger\ell_\alpha + M_i N_i \tilde{N}_i \\
& + \frac{y_i}{2}S^\dagger N_i N_i + \frac{\tilde{y}_i}{2}S\tilde{N}_i\tilde{N}_i + \text{h.c.}, \\
V = {} & \lambda_1(\phi^\dagger\phi)^2 + \lambda_2(\eta^\dagger\eta)^2 + \lambda_3(\phi^\dagger\phi)(\eta^\dagger\eta) \\
& + \lambda_4(\eta^\dagger\phi)(\phi^\dagger\eta) + \frac{\lambda_5'}{2}\left[\frac{S}{M_*}(\phi^\dagger\eta)^2 + \text{h.c.}\right] \\
& + \lambda_6(S^\dagger S)(\phi^\dagger\phi) + \lambda_7(S^\dagger S)(\eta^\dagger\eta) + \kappa(S^\dagger S)^2 \\
& + m_\phi^2\phi^\dagger\phi + m_\eta^2\eta^\dagger\eta + m_S^2 S^\dagger S,
\end{aligned}
\tag{1}
$$

where ℓ_α is a left-handed doublet lepton and ϕ is an ordinary doublet Higgs scalar. M_* is a cut-off scale of this model. The bare masses M_i and m_η in Eq. (1) are assumed to be real and of $O(1)$ TeV. The couplings $h_{\alpha i}$ and $f_{\alpha i}$ in the neutrino

sector are considered to be written by using the basis in which the Yukawa coupling matrix of charged leptons is diagonal. As easily found in Eq. (1), if the singlet S has a vacuum expectation value, the coupling λ_5 in the original Ma model and neutrino Yukawa couplings $\tilde{h}_{\alpha i}$ for $\tilde{N}_i$ are determined as [23,24]

$$
\lambda_5 = \lambda_5'\frac{\langle S \rangle}{M_*}, \quad \tilde{h}_{\alpha i} = f_{\alpha i}\frac{\langle S^\dagger \rangle}{M_*},
\tag{2}
$$

where it may be natural to consider that both λ_5' and $f_{\alpha i}$ are of $O(1)$. The magnitude of λ_5 is crucial for the neutrino mass determination in the model. We note that it can be small enough if $|\langle S \rangle| \ll M_*$ is satisfied. Scales assumed for $|\langle S \rangle|$ and M_* in the present study are discussed below.

2.2 Scalar sector

First, we discuss the scalar sector of the model. We express the scalar fields by using a unitary gauge,

$$
\phi^T = \left(0, \langle\phi\rangle + \frac{h}{\sqrt{2}}\right), \quad \eta^T = \left(\eta^+, \frac{1}{\sqrt{2}}(\eta_R + i\eta_I)\right),
$$
$$
S = \langle S \rangle + \frac{\sigma}{\sqrt{2}},
\tag{3}
$$

where both vacuum expectation values $\langle\phi\rangle$ and $\langle S \rangle$ are assumed to be real and positive. In this vacuum, the new Abelian gauge boson X_μ gets a mass $m_X^2 = 2g_X^2\langle S \rangle^2$. The scalar potential V in Eq. (1) can be represented by using Eq. (3) as

$$
\begin{aligned}
V = {} & \frac{1}{2}(4\lambda_1\langle\phi\rangle^2 h^2 + 4\kappa\langle S \rangle^2\sigma^2 + 4\lambda_6\langle\phi\rangle\langle S\rangle h\sigma) \\
& + \frac{1}{2}M_{\eta_R}^2\eta_R^2 + \frac{1}{2}M_{\eta_I}^2\eta_I^2 + M_{\eta_c}^2\eta^+\eta^- \\
& + \frac{1}{4}\left[\sqrt{\lambda_1}h^2 - \sqrt{\lambda_2}(2\eta^+\eta^- + \eta_R^2 + \eta_I^2) - \sqrt{\kappa}\sigma^2\right]^2 \\
& + \frac{1}{4}\Big[\Big\{2(\lambda_3 + 2\sqrt{\lambda_1\lambda_2})\eta^+\eta^- \\
& + (\lambda_+ + 2\sqrt{\lambda_1\lambda_2})\eta_R^2 + (\lambda_- + 2\sqrt{\lambda_1\lambda_2})\eta_I^2 \\
& + (\lambda_6 + 2\sqrt{\lambda_1\kappa})\sigma^2\Big\}h^2 \\
& + (\lambda_7 - 2\sqrt{\lambda_2\kappa})(2\eta_+\eta_- + \eta_R^2 + \eta_I^2)\sigma^2\Big] \\
& + \sqrt{2}\lambda_1\langle\phi\rangle h^3 + \sqrt{2}\kappa\langle S\rangle\sigma^3 \\
& + \sqrt{2}(\lambda_3\langle\phi\rangle h + \lambda_7\langle S\rangle\sigma)\eta_+\eta_- \\
& + \frac{1}{\sqrt{2}}(\lambda_+\langle\phi\rangle h + \lambda_7\langle S\rangle\sigma)\eta_R^2 \\
& + \frac{1}{\sqrt{2}}(\lambda_-\langle\phi\rangle h + \lambda_7\langle S\rangle\sigma)\eta_I^2 + \frac{\lambda_6}{\sqrt{2}}(\langle\phi\rangle h\sigma^2 + \langle S\rangle\sigma h^2) \\
& + \frac{\lambda_5'}{4\sqrt{2}M_*}\sigma h^2(\eta_R^2 - \eta_I^2),
\end{aligned}
\tag{4}
$$

where we use the definition $\lambda_\pm = \lambda_3 + \lambda_4 \pm \lambda_5$ and

$$
M_{\eta_c}^2 = m_\eta^2 + \lambda_7 \langle S \rangle^2 + \lambda_3 \langle \phi \rangle^2,
$$
$$
M_{\eta_{R(I)}}^2 = m_\eta^2 + \lambda_7 \langle S \rangle^2 + \lambda_{+(-)} \langle \phi \rangle^2. \tag{5}
$$

The difference between these masses is estimated to be

$$
\frac{M_{\eta_I} - M_{\eta_R}}{M_{\eta_R}} \simeq \frac{\lambda_5 \langle \phi \rangle^2}{M_{\eta_R}^2} \equiv \frac{\delta}{M_{\eta_R}},
$$
$$
\frac{M_{\eta_c} - M_{\eta_R}}{M_{\eta_R}} \simeq \frac{(\lambda_4 + \lambda_5) \langle \phi \rangle^2}{2 M_{\eta_R}^2}, \tag{6}
$$

which could be a good approximation as long as $m_\eta^2 + \lambda_7 \langle S \rangle^2 \gg \langle \phi \rangle^2$ is satisfied. A large value of $m_\eta^2 + \lambda_7 \langle S \rangle^2$ is favored from the analysis of the T parameter in precise measurements of the electroweak interaction [47–55]. We assume such a situation in the present study.

Quartic scalar couplings in the potential V are constrained by several conditions. The stability of the assumed vacuum requires

$$
\lambda_1, \lambda_2, \kappa > 0; \quad \lambda_3, \lambda_\pm > -2\sqrt{\lambda_1 \lambda_2}; \quad \lambda_6 > -2\sqrt{\lambda_1 \kappa};
$$
$$
\lambda_7 > -2\sqrt{\lambda_2 \kappa}. \tag{7}
$$

These can be easily read off from the expression of the scalar potential V given in Eq. (4).[1] Perturbativity of the model imposes that these quartic couplings should be smaller than 4π.[2] Moreover, if we assume that η_R is the lightest one among the fields with odd parity of the remnant Z_2, Eq. (5) shows that the following conditions should be satisfied:

$$
\lambda_4 + \lambda_5 < 0, \quad \lambda_5 < 0; \quad M_{\eta_R} < \min(M_{\pm i}), \tag{8}
$$

where $M_{\pm i}$ are the mass eigenvalues for N_i and $\tilde{N}_i$, which are discussed in detail later. Using the value of λ_1 predicted by the Higgs mass observed at LHC experiments [1,2] and the conditions given in Eqs. (7) and (8), we can roughly estimate the allowed range of $\lambda_{3,4}$ as

$$
-2.5 < \lambda_3 < 4\pi, \quad -4\pi < \lambda_4 < 0, \tag{9}
$$

for sufficiently small values of $|\lambda_5|$.

The potential minimum in Eq. (4) is obtained as

$$
\langle \phi \rangle^2 = \frac{\lambda_6 m_S^2 - 2\kappa m_\phi^2}{4\lambda_1 \kappa - \lambda_6^2}, \quad \langle S \rangle^2 = \frac{\lambda_6 m_\phi^2 - 2\lambda_1 m_S^2}{4\lambda_1 \kappa - \lambda_6^2}. \tag{10}
$$

Since the new gauge boson does not couple with the standard model fields, both cases $\langle S \rangle^2 \gg \langle \phi \rangle^2$ and $\langle S \rangle^2 \ll \langle \phi \rangle^2$ could be phenomenologically allowed. However, if we apply this model to the leptogenesis, $\langle S \rangle^2 \gg \langle \phi \rangle^2$ should be satisfied

---

[1] The last condition can be found by using a different expression of V, which is modified so that $\sqrt{\kappa}$ has the opposite sign to Eq. (4).

[2] More precisely, $|\lambda_{1,2}|$ and $|\kappa|$ should be smaller than $\frac{2\pi}{3}$.

as discussed later. Such a vacuum can be realized for a sufficiently small $|\lambda_6|$ satisfying $4\lambda_1 \kappa \gg \lambda_6^2$ and negative values of m_S^2 and m_ϕ^2 satisfying $|m_S^2| \gg |m_\phi^2|$. In this case, both vacuum expectation values are approximately expressed as $\langle \phi \rangle^2 \simeq -\frac{m_\phi^2}{2\lambda_1}$ and $\langle S \rangle^2 \simeq -\frac{m_S^2}{2\kappa}$. If the contribution of $\langle S \rangle$ to the η mass is of the same order as that of $\langle \phi \rangle$, $|\lambda_7|$ should be much smaller than $|\lambda_{3,4}|$ as found from Eq. (5).

Since h and σ defined in Eq. (3) have mass mixing as found from the first line in Eq. (4), the mass eigenstates $\tilde{h}$ and $\tilde{\sigma}$ are a mixture of these. They are found to enable us to write

$$
\tilde{h} \simeq h - \frac{\lambda_6 \langle \phi \rangle}{2\kappa \langle S \rangle} \sigma, \quad \tilde{\sigma} = \sigma + \frac{\lambda_6 \langle \phi \rangle}{2\kappa \langle S \rangle} h. \tag{11}
$$

However, since $\langle S \rangle^2 \gg \langle \phi \rangle^2$ is assumed and $|\lambda_6| < \sqrt{\kappa}$ is expected, the mass eigenstates could be almost equal to h and σ. In this case, the mass eigenvalues are approximately expressed as

$$
m_{\tilde{h}}^2 = \left(4\lambda_1 - \frac{\lambda_6^2}{\kappa} \right) \langle \phi \rangle^2, \quad M_{\tilde{\sigma}}^2 \simeq 4\kappa \langle S \rangle^2. \tag{12}
$$

These should have positive values for the stability of the considered vacuum. It requires $4\lambda_1 \kappa > \lambda_6^2$, which is consistent with the above discussion.

The value of λ_1 might be estimated by using $m_{\tilde{h}} \simeq 125$ GeV. If we apply it to the tree-level formula in Eq. (12), we have

$$
\lambda_1 - \frac{\lambda_6^2}{4\kappa} \sim 0.13. \tag{13}
$$

This result suggests that λ_1 could have a somewhat larger value than the corresponding quartic coupling in the standard model. However, this effect is expected to be small since the assumed vacuum requires $4\lambda_1 \kappa \gg \lambda_6^2$. On the other hand, the model has the additional scalar couplings λ_3 and λ_4, which are known to improve the potential stability [56,57]. Thus, the constraint from the potential stability against the radiative correction in the present model could be milder than that of the standard model.

If we impose the requirement that $\tilde{\sigma}$ is heavier than the Higgs scalar, κ satisfies $\kappa \gtrsim 10^{-3} \left(\frac{2\,\text{TeV}}{\langle S \rangle} \right)^2$ and λ_6 could take a small value so as to be consistent with the condition $|\lambda_6| < 2\sqrt{\lambda_1 \kappa}$. If the above condition for κ is not satisfied, $\tilde{\sigma}$ can be lighter than $\tilde{h}$ so as to realize $m_{\tilde{h}} > 2M_{\tilde{\sigma}}$. In that case, the coupling λ_6 satisfies $|\lambda_6| \lesssim 10^{-2} \left(\frac{\lambda_1}{0.13} \right)^{\frac{1}{2}} \left(\frac{2\,\text{TeV}}{\langle S \rangle} \right)$ and the interaction in the last line of Eq. (4) induces the invisible decay $\tilde{h} \to 2\tilde{\sigma}$. The decay width can be estimated as

$$\Gamma(\tilde{h} \to 2\tilde{\sigma}) = \frac{\lambda_6^2 |\langle \phi \rangle|^2}{16\pi m_{\tilde{h}}} \sqrt{1 - 4\frac{M_{\tilde{\sigma}}^2}{m_{\tilde{h}}^2}}. \tag{14}$$

The branching ratio of this invisible decay should be less than 19 % of the Higgs total width $\sim$4 MeV [58]. This constrains the value of λ_6 as $|\lambda_6| < 0.0126$ [59], which could be consistent with the vacuum condition discussed above. Here, we note that both κ and λ_6 take small values for the light $\tilde{\sigma}$. In that case, $\tilde{\sigma}$ could have non-negligible cosmological effects. We will come back to this point later.

2.3 Degenerate right-handed neutrinos

Next, we discuss the neutrino sector. If the thermal leptogenesis at TeV scales is supposed to be the origin of baryon number asymmetry in the Universe, the mass degeneracy among right-handed neutrinos is indispensable, at least in certain parameter regions [31,32]. In the present model, spontaneous breaking of a new Abelian gauge symmetry due to a vacuum expectation value of S could make the singlet fermions N_i and $\tilde{N}_i$ behave as pseudo-Dirac fermions. In fact, if $|y_i \langle S^\dagger \rangle|, |\tilde{y}_i \langle S \rangle| \ll M_i$ is satisfied, their masses are almost degenerate.[3]

The mass matrix of the singlet fermions is expressed as

$$\frac{1}{2}(N_i, \tilde{N}_i) \begin{pmatrix} |y_i| e^{i\gamma_i} \langle S^\dagger \rangle & M_i \\ M_i & |\tilde{y}_i| e^{i\tilde{\gamma}_i} \langle S \rangle \end{pmatrix} \begin{pmatrix} N_i \\ \tilde{N}_i \end{pmatrix} + \text{h.c.}, \tag{15}$$

where M_i and $\langle S \rangle$ can be taken to be positive generally. The mass eigenvalues $M_{\pm i}$ are derived as

$$\begin{aligned} M_{+i} &\simeq M_i \sin 2\theta_i + (|y_i| \cos(\gamma_i - \xi_i) \cos^2 \theta_i \\ &\quad + |\tilde{y}_i| \cos(\tilde{\gamma}_i + \xi_i) \sin^2 \theta_i) \langle S \rangle, \\ M_{-i} &\simeq M_i \sin 2\theta_i - (|y_i| \cos(\gamma_i - \xi_i) \sin^2 \theta_i \\ &\quad + |\tilde{y}_i| \cos(\tilde{\gamma}_i + \xi_i) \cos^2 \theta_i) \langle S \rangle, \end{aligned} \tag{16}$$

and the corresponding mass eigenstates $\mathcal{N}_{\pm i}$ are found to enable us to write

$$\begin{aligned} \mathcal{N}_{+i} &= e^{-i\frac{\xi_i}{2}}(N_i \cos \theta_i + \tilde{N}_i e^{-i\xi_i} \sin \theta_i), \\ \mathcal{N}_{-i} &= i e^{-i\frac{\xi_i}{2}}(-N_i \sin \theta_i + \tilde{N}_i e^{-i\xi_i} \cos \theta_i), \end{aligned} \tag{17}$$

respectively. Here, the phase ξ_i is fixed by the parameters in the mass matrix as

$$\tan \xi_i = \frac{|y_i| \sin \gamma_i - |\tilde{y}_i| \sin \tilde{\gamma}_i}{|y_i| \cos \gamma_i + |\tilde{y}_i| \cos \tilde{\gamma}_i}, \tag{18}$$

and the mixing angle θ_i is given by using this ξ_i as

$$\tan 2\theta_i = \frac{M_i}{\langle S \rangle} \frac{2}{|y_i| \cos(\gamma_i - \xi_i) - |\tilde{y}_i| \cos(\tilde{\gamma}_i + \xi_i)}. \tag{19}$$

The difference of the mass eigenvalues given in Eq. (16) is expressed by using these, thus:

$$\Delta_i \equiv \frac{M_{+i} - M_{-i}}{M_{-i}} \simeq \frac{\langle S \rangle}{M_i} \frac{|y_i| \cos(\gamma_i - \xi_i) + |\tilde{y}_i| \cos(\tilde{\gamma}_i + \xi_i)}{\sin 2\theta_i}. \tag{20}$$

From these formulas, we find that θ_i could be approximated as $\frac{\pi}{4}$ and also the right-handed neutrino masses might be finely degenerate at a period where the sphaleron interaction is in thermal equilibrium, simultaneously. The condition required for this is that both $|y_i| \langle S \rangle$ and $|\tilde{y}_i| \langle S \rangle$ are much smaller than M_i which is assumed to be of $O(1)$ TeV. This implies that the resonant leptogenesis could occur for a value of $\langle S \rangle$ which is larger than the weak scale as long as both $|y_i|$ and $|\tilde{y}_i|$ are sufficiently small.

The neutrino Yukawa couplings and other relevant interactions of the right-handed neutrinos in Eq. (1) can be written by using the mass eigenstates $\mathcal{N}_{\pm i}$, thus

$$\begin{aligned} \sum_{i=1,2} &\Bigg[e^{-i\frac{\xi_i}{2}} \Big(h_{\alpha i} \cos \theta_i + \tilde{h}_{\alpha i} e^{-i\xi_i} \sin \theta_i \Big) \bar{\mathcal{N}}_{+i} \eta^\dagger \ell_\alpha \\ &- i e^{-i\frac{\xi_i}{2}} \Big(h_{\alpha i} \sin \theta_i - \tilde{h}_{\alpha i} e^{-i\xi_i} \cos \theta_i \Big) \bar{\mathcal{N}}_{-i} \eta^\dagger \ell_\alpha \\ &+ \frac{1}{2\sqrt{2}} \Big\{ \Big(|y_i| e^{i(\gamma_i + \xi_i)} \cos^2 \theta_i + |\tilde{y}_i| e^{i(\tilde{\gamma}_i + 3\xi_i)} \sin^2 \theta_i \Big) \tilde{\sigma} \mathcal{N}_{+i}^2 \\ &- \Big(|y_i| e^{i(\gamma_i + \xi_i)} \sin^2 \theta_i + |\tilde{y}_i| e^{i(\tilde{\gamma}_i + 3\xi_i)} \cos^2 \theta_i \Big) \tilde{\sigma} \mathcal{N}_{-i}^2 \\ &+ i \sin 2\theta_i \Big(|y_i| e^{i(\gamma_i + \xi_i)} - |\tilde{y}_i| e^{i(\tilde{\gamma}_i + 3\xi_i)} \Big) \tilde{\sigma} \mathcal{N}_{+i} \mathcal{N}_{-i} \Big\} \\ &+ i g_X \sin 2\theta_i \, X_\mu (\bar{\mathcal{N}}_{+i} \gamma^\mu \mathcal{N}_{-i}) + \text{h.c.} \Bigg]. \end{aligned} \tag{21}$$

If $h_{\alpha i} = \tilde{h}_{\alpha i}$ is satisfied,[4] the flavor structure of the model becomes very simple. In that case, the neutrino Yukawa couplings can be rewritten as

$$\begin{aligned} g_{\alpha i}^{(+)} &\equiv e^{-i\frac{\xi_i}{2}} h_{\alpha i} (\cos \theta_i + e^{-i\xi_i} \sin \theta_i) \\ &= h_{\alpha i} (1 + \cos \xi_i \sin 2\theta_i)^{\frac{1}{2}} e^{i(\delta_{+i} - \frac{\xi_i}{2})}, \\ g_{\alpha i}^{(-)} &\equiv -i e^{-i\frac{\xi_i}{2}} h_{\alpha i} (\sin \theta_i - e^{-i\xi_i} \cos \theta_i) \\ &= h_{\alpha i} (1 - \cos \xi_i \sin 2\theta_i)^{\frac{1}{2}} e^{i(\delta_{-i} - \frac{\xi_i}{2})}, \end{aligned} \tag{22}$$

---

[3] The same scenario has been considered to explain the mass degeneracy among right-handed neutrinos first in [44]. It is also discussed in [60,61], for example.

[4] Although this assumption is not necessary for the present scenario, we adopt it to make the analysis easier.

where we suppose $h_{\alpha i}$ to be real, for simplicity. The phases $\delta_{\pm i}$ are defined as

$$\tan \delta_{+i} = \frac{-\sin \xi_i \tan \theta_i}{1 + \cos \xi_i \tan \theta_i}, \quad \cot \delta_{-i} = \frac{\sin \xi_i}{\cos \xi_i - \tan \theta_i}. \tag{23}$$

We use these simplified neutrino Yukawa couplings in the following discussion.

The neutrino mass is induced through one-loop diagrams which have $\mathcal{N}_{+i}$ or $\mathcal{N}_{-i}$ in an internal fermion line as in the original model. The mass formula is given by

$$\mathcal{M}_{\alpha\beta} = \sum_i \sum_{s=\pm} |g_{\alpha i}^{(s)} g_{\beta i}^{(s)} \lambda_5| e^{i(2\delta_{si} - \xi_i)} \Lambda(M_{si}), \tag{24}$$

where $\Lambda(M_{\pm i})$ is defined as

$$\Lambda(M_{\pm i}) = \frac{\langle \phi \rangle^2}{8\pi^2} \frac{M_{\pm i}}{M_\eta^2 - M_{\pm i}^2} \left(1 + \frac{M_{\pm i}^2}{M_\eta^2 - M_{\pm i}^2} \ln \frac{M_{\pm i}^2}{M_\eta^2} \right). \tag{25}$$

M_η is an averaged value of the mass eigenvalues of η_R and η_I. If the model has two sets of $(N_i, \tilde{N}_i)$ at least, neutrino mass eigenvalues suitable for the explanation of the neutrino oscillation data could be derived.[5] We consider a model with two sets of $(N_i, \tilde{N}_i)$ in the following.

Since the scale $\Lambda(M_{\pm i})$ is estimated as $\Lambda(M_{\pm i}) = O(10^9)$ eV for η and $\mathcal{N}_{\pm i}$ whose masses are in the TeV range, Eq. (24) suggests that the atmospheric neutrino data require the relevant neutrino Yukawa couplings to satisfy

$$\sum_i |g_{\alpha i}^{(\pm)} g_{\beta i}^{(\pm)} \lambda_5| = O(10^{-11}). \tag{26}$$

On the other hand, if $\mathcal{N}_{-1}$ is identified with the lightest right-handed neutrino, its decay should occur in out-of-thermal equilibrium for successful leptogenesis. This condition could impose strong constraints on various interactions of $\mathcal{N}_{-1}$. They can be roughly estimated by imposing both reaction rates of the decay of $\mathcal{N}_{-1}$ and its scattering with other particles to be smaller than the Hubble parameter. The most important process is the $\mathcal{N}_{-1}$ decay. If the neutrino Yukawa couplings of $\mathcal{N}_{-1}$ satisfy

$$\left(\sum_\alpha \left| g_{\alpha 1}^{(-)} \right|^2 \right)^{\frac{1}{2}} \leq 10^{-8}, \tag{27}$$

it does not reach equilibrium at the temperature $T \gtrsim 100$ GeV.

---

[5] We can consider another minimal model which has one set of $(N_1, \tilde{N}_1)$ and an additional right-handed neutrino which has no charge of $U(1)_X$. A result similar to the present one could be expected for neutrino masses and leptogenesis also in such a model.

The condition (27) shows that $\mathcal{N}_{-1}$ causes a negligible contribution to the neutrino mass generation, which is found from Eqs. (24) and (26). On the other hand, if $\mathcal{N}_{+1}$ is supposed to cause a main contribution to the neutrino mass generation, the condition (26) shows that its Yukawa couplings should satisfy

$$|g_{\alpha 1}^{(+)}|^2 = O\left(\frac{10^{-11}}{|\lambda_5|} \right) \quad (\alpha = e, \mu, \tau). \tag{28}$$

Equation (22) suggests that the original neutrino Yukawa couplings $|h_{\alpha 1}|$ do not need to be extremely small for the simultaneous realization of the conditions (27) and (28), as long as $\cos \xi_1 \sin 2\theta_1 \simeq 1$ is satisfied to a good accuracy and also $|\lambda_5|$ takes a small value of $O(10^{-4})$. Other nonzero neutrino mass eigenvalues could be determined through the second pair $(N_2, \tilde{N}_2)$. Since the relevant Yukawa couplings $h_{\alpha 2}$ are not constrained by the leptogenesis, we can derive neutrino masses and mixing favorable for the explanation of the neutrino oscillation data through Eq. (24) independently. If only one of $\mathcal{N}_{\pm 2}$ contributes to the neutrino mass generation as in the $(N_1, \tilde{N}_1)$ sector, one of three neutrino mass eigenvalues is expected to be negligibly small as in the model studied in [31,32].

2.4 Resonant leptogenesis

In this framework, we consider resonant leptogenesis [37–44]. The dominant contribution to the CP asymmetry ε in the $\mathcal{N}_{-1}$ decay comes from the resonance appearing in the one-loop self-energy diagram. In that case, ε is known to enable us to express it as [41–44]

$$\begin{aligned} \varepsilon &= \frac{\mathrm{Im}\left(\sum_\alpha g_{\alpha 1}^{(+)*} g_{\alpha 1}^{(-)} \right)^2}{\left(\sum_\alpha g_{\alpha 1}^{(-)*} g_{\alpha 1}^{(-)} \right) \left(\sum_\alpha g_{\alpha 1}^{(+)*} g_{\alpha 1}^{(+)} \right)} \frac{2\Delta_1 \tilde{\Gamma}_{\mathcal{N}_{+1}}}{4\Delta_1^2 + \tilde{\Gamma}_{\mathcal{N}_{+1}}^2} \\ &= \frac{\cos 2\theta_1 \sin 2\xi_1}{1 - \sin^2 2\theta_1 \cos^2 \xi_1} \frac{2\Delta_1 \tilde{\Gamma}_{\mathcal{N}_{+1}}}{4\Delta_1^2 + \tilde{\Gamma}_{\mathcal{N}_{+1}}^2}, \end{aligned} \tag{29}$$

where we use the expression of the neutrino Yukawa couplings $|g_{\alpha 1}^\pm|$ given in Eq. (22). The mass degeneracy Δ_1 is defined in Eq. (20) and $\tilde{\Gamma}_{\mathcal{N}_{+1}} = \frac{\sum_\alpha \left| g_{\alpha 1}^{(+)} \right|^2}{8\pi} \left(1 - \frac{M_\eta^2}{M_{+1}^2} \right)^2$. If we assume $\langle S \rangle = M_1$ for simplicity, the right-handed neutrino sector $(N_1, \tilde{N}_1)$ has five free parameters. Using these, we study the relation between the CP asymmetry and the structure of right-handed neutrino sector.

In Fig. 1, we plot the CP asymmetry ε as a function of γ_1 for four typical sets of $(|y_1|, |h_{\alpha 1}|)$. Other parameters are fixed at the values given in the caption of Fig. 1. We find that ε changes the sign from minus to plus at $\gamma_1 \sim 10^{-4}$ and 5×10^{-5} for the cases A, B and C, D, respectively. Its absolute value is enhanced largely around these values of γ_1.
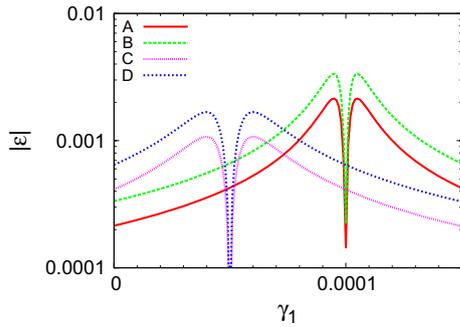
Fig. 1 CP asymmetry as a function of γ_1 for typical values of $(|y_1|, |h_{\alpha 1}|)$. In each case, these parameters are fixed as A(10^{-5}, 4×10^{-4}), B(10^{-5}, 5×10^{-4}), C(2×10^{-5}, 4×10^{-4}), and D(2×10^{-5}, 5×10^{-4}). Other relevant parameters are taken to be $\tilde{\gamma}_1 = 0.1$, $\tilde{y}_1 = 10^{-8}$, $M_1 = \langle S \rangle = 2$ TeV and $M_\eta = 1$ TeV

If we note that $|g_{\alpha 1}^{(-)}| \leq O(10^{-8})$ is required for the out-of-equilibrium decay of $\mathcal{N}_{-1}$, we find that $|\xi_1|$ should take a very small value such as $O(10^{-4})$ for $|h_{\alpha 1}| = O(10^{-4})$. As found from Eq. (18), such a small $|\xi_1|$ could be easily realized for hierarchical $|y_1|$ and $|\tilde{y}_1|$ by fixing the values of γ_1 and $\tilde{\gamma}_1$ appropriately. In these examples, such hierarchical values are assumed for $|y_1|$ and $|\tilde{y}_1|$. We also note that the same parameter set could induce the degenerate right-handed neutrino masses as found from Eq. (20). This feature makes it for the model possible to satisfy the minimum conditions for the success of resonant leptogenesis. Although we have to introduce a tiny coupling $|\tilde{y}_1|$ in this scenario, the important quantities for the leptogenesis are closely related each other. The model can bring about their favorable values simultaneously based on the common parameters. In fact, for the parameters used in Fig. 1, the desirable values of the relevant quantities to the leptogenesis can be obtained. We present their values derived from these parameters in Table 1. These results show that $|g_{\alpha 1}^{(-)}|$ takes small values which satisfy the condition (28) at the points where the CP asymmetry $|\varepsilon|$ has large values. The mass degeneracy $\Delta_1 = O(10^{-5})$ between the right-handed neutrinos $\mathcal{N}_{\pm 1}$ is also realized at this region. This level of degeneracy has been shown to be sufficient for the leptogenesis in the radiative neutrino mass model in the previous study [31,32]. Although the smallness

Table 1 Derived values of the quantities relevant to the leptogenesis for each case given in Fig. 1. These are estimated at $\gamma_1 \sim 9 \times 10^{-5}$ and 4×10^{-5} for the cases A, B and C, D, respectively

|	$|g_{\alpha 1}^{(-)}|$	$|g_{\alpha 1}^{(+)}|$	Δ_1	ε
A	3.12×10^{-9}	5.66×10^{-4}	1.00×10^{-5}	-1.73×10^{-3}
B	6.71×10^{-9}	7.07×10^{-4}	1.00×10^{-5}	-2.71×10^{-3}
C	1.17×10^{-8}	5.66×10^{-4}	2.00×10^{-5}	-5.04×10^{-4}
D	1.46×10^{-8}	7.07×10^{-4}	2.00×10^{-5}	-7.88×10^{-4}

of $|\tilde{y}_1|$ should be explained by considering some complete model in the high energy region, it is beyond the scope of the present study and we do not go further in this direction here.

The baryon number asymmetry generated through the decay of $\mathcal{N}_{-1}$ can be fixed by estimating the generated lepton number asymmetry through solving the Boltzmann equations numerically for both the $\mathcal{N}_{-1}$ number density $n_{\mathcal{N}_{-1}}$ and the lepton number asymmetry $n_L (\equiv n_\ell - n_{\bar{\ell}})$. We introduce these number densities in the co-moving volume as $Y_{\mathcal{N}_{-1}} = \frac{n_{\mathcal{N}_{-1}}}{s}$ and $Y_L = \frac{n_L}{s}$ by using the entropy density s. The Boltzmann equations for these are written as

$$
\begin{aligned}
\frac{dY_{\mathcal{N}_{-1}}}{dz} &= -\frac{z}{sH(M_{-1})} \left(\frac{Y_{\mathcal{N}_{-1}}}{Y_{\mathcal{N}_{-1}}^{eq}} - 1 \right) \\
&\quad \times \{ \gamma_{\mathcal{N}_{-1}}^D + \gamma_{\mathcal{N}_{-1}\tilde{\sigma}}^S + \gamma_{\mathcal{N}_{-1}X}^S \}, \\
\frac{dY_L}{dz} &= \frac{z}{sH(M_{-1})} \left\{ \varepsilon \left(\frac{Y_{\mathcal{N}_{-1}}}{Y_{\mathcal{N}_{-1}}^{eq}} - 1 \right) \gamma_{\mathcal{N}_{-1}}^D - \frac{2Y_L}{Y_\ell^{eq}} \right. \\
&\quad \left. \times \left(\frac{\gamma_{\mathcal{N}_{+1}}^D}{4} + \gamma_{\mathcal{N}_{+1}}^{(2)} + \gamma_{\mathcal{N}_{+1}}^{(13)} \right) \right\},
\end{aligned}
\tag{30}
$$

where $z = \frac{M_{-1}}{T}$ and $H(M_{-1}) = 1.66 g_*^{1/2} \frac{M_{-1}^2}{m_{pl}}$. The equilibrium values for these are expressed as $Y_{\mathcal{N}_{-1}}^{eq}(z) = \frac{45}{2\pi^4 g_*} z^2 K_2(z)$ and $Y_\ell^{eq} \simeq \frac{81}{\pi^4 g_*}$, where $K_2(z)$ is the modified Bessel function of the second kind. Since the Yukawa couplings of $\mathcal{N}_{+1}$ are large enough, it is expected to be in thermal equilibrium throughout the relevant period. In these equations, we take into account the important reactions which could keep $\mathcal{N}_{-1}$ in the equilibrium and wash out the generated lepton number asymmetry. The former ones include the 2–2 scatterings of $\mathcal{N}_{-1}$ with $\tilde{\sigma}$ and X_μ, whose reaction densities are represented by $\gamma_{\mathcal{N}_{-1}\tilde{\sigma}}^S$ and $\gamma_{\mathcal{N}_{-1}X}^S$ in Eq. (30). These could be effective if $\tilde{\sigma}$ and X_μ are light enough. Other reaction densities in Eq. (30) can be found in the appendix of [31,32].

In Fig. 2, the solutions of these equations and the reaction rates Γ of the relevant processes are plotted as functions of z for the case A in Table 1. In these panels, the masses of $\tilde{\sigma}$ and X_μ are fixed to be $(M_{\tilde{\sigma}}, m_X) = (200, 300)$, $(60, 100)$, and $(200, 10^{-3})$ in GeV units, respectively. As the initial condition for $Y_{\mathcal{N}_{-1}}$ in the Boltzmann equations we use its equilibrium value, since both N_1 and $\tilde{N}_1$ are expected to be in thermal equilibrium. Since we adopt this initial condition, its deviation $\Delta_{\mathcal{N}_{-1}}$ from the equilibrium value does not change sign as found in the upper panels of this figure. After $\langle S \rangle$ becomes nonzero, the mass eigenstate $\mathcal{N}_{-1}$ leaves the equilibrium because of its small Yukawa coupling $g_{\alpha 1}^{(-)}$. Thus, it could be crucial in the estimation of the lepton number asymmetry at what value of z we introduce the effect of nonzero $\langle S \rangle$ in the equations. As a simple approximation,
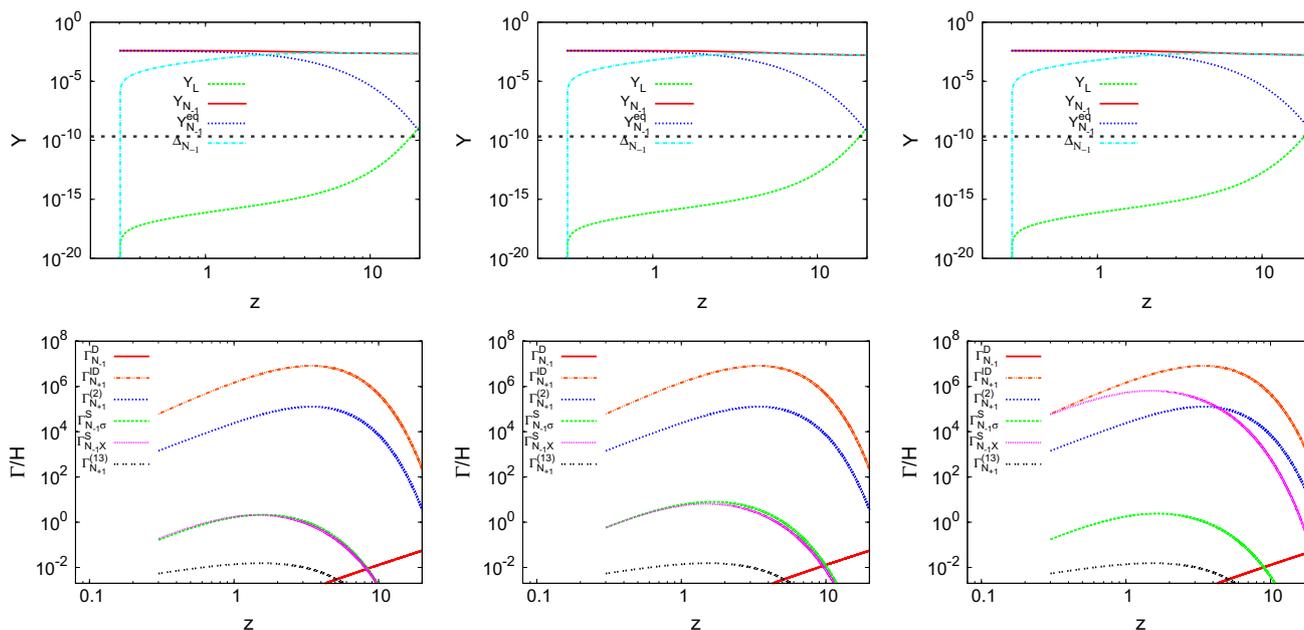
Fig. 2 In the *upper panels*, solutions of the Boltzmann equations are plotted as a function of z for the case A shown in Table 1. In the *lower panels*, relevant reaction rates Γ/H are plotted as a function of z for the same parameters used in the corresponding *upper panels*. Reaction rates of the $\mathcal{N}_{-1}$ decay, the $\mathcal{N}_{+1}$ inverse decay, and the lep-ton number violating $\mathcal{N}_{+1}$ scatterings are represented by $\Gamma^D_{N_{-1}}$, $\Gamma^{ID}_{N_{+1}}$ and $\Gamma^{(2)}_{N_{+1}}$, $\Gamma^{(13)}_{N_{+1}}$, respectively. The masses of $\tilde{\sigma}$ and X_μ are set as $(M_{\tilde{\sigma}}, m_X) = (200, 300)$, $(60, 100)$, and $(200, 10^{-3})$ in GeV units from *left* to *right*, respectively

we introduce its effect as a step function at z_0. In order to check the validity of this analysis, we change the value of z_0 in the range $0.3 < z_0 < 1$ to examine the z_0 dependence of the final results. Since their difference stays at most in a few 10 % range without showing a serious z_0 dependence, the present treatment can be considered to give reliable results.

In the lower panels, which plot the behavior of the reaction rates, we find that the inverse decay of $\mathcal{N}_{+1}$ plays a dominant role for the wash-out of the generated lepton number asymmetry among various processes. Although the $\mathcal{N}_{+1}$ mass is almost degenerate with the mass of $\mathcal{N}_{-1}$, its Yukawa coupling $g^{(+)}_{\alpha 1}$ is not so small as to decouple at an earlier period. This is an expected feature in the resonant leptogenesis generally. The rapid increase of the lepton number asymmetry shown in the $z > 10$ region can be understood from the large decrease of $\Gamma^{ID}_{N_{+1}}$ there. The scatterings of $\mathcal{N}_{-1}$ with $\tilde{\sigma}$ and X_μ cannot be effective in keeping $\mathcal{N}_{-1}$ in thermal equilibrium even if $\tilde{\sigma}$ and X_μ are light enough. Since $\langle S \rangle$ is supposed to be rather large, the assumed masses for $\tilde{\sigma}$ and X_μ are obtained only for the small couplings κ and g_X. This is considered to be the cause of these results.

The baryon number asymmetry $Y_B (\equiv \frac{n_B}{s})$ is expressed by using the solution Y_L of the Boltzmann equations, thus

$$Y_B = -\frac{8}{23} Y_L(z_{EW}),$$
(31)

Table 2 Baryon number asymmetry Y_B predicted for the parameter sets given in Table 1. $M_{\tilde{\sigma}}$ and m_X are given in GeV units

$(M_{\tilde{\sigma}}, m_X)$	A	B	C	D
$(200, 300)$	5.2×10^{-10}	2.3×10^{-9}	4.2×10^{-10}	5.6×10^{-10}
$(60, 100)$	3.9×10^{-10}	1.7×10^{-9}	1.5×10^{-10}	1.9×10^{-10}
$(200, 10^{-3})$	4.0×10^{-10}	1.8×10^{-9}	1.6×10^{-10}	2.2×10^{-10}
$(600, 600)$	7.0×10^{-10}	3.1×10^{-9}	1.1×10^{-9}	1.4×10^{-9}

where z_{EW} is related to the sphaleron decoupling temperature T_{EW} by $z_{EW} = \frac{M_{-1}}{T_{EW}}$. The baryon number asymmetry predicted for the parameters given in Table 1 is listed in Table 2 for several values of $(M_{\tilde{\sigma}}, m_X)$. These results show that the model could generate the sufficient baryon number asymmetry compared with $8.1 \times 10^{-11} < Y_B < 9.2 \times 10^{-11}$ (95 % CL) required from the observation [45] as long as the relevant parameters take suitable values.[6] We note that the light $\tilde{\sigma}$ which can contribute to the invisible decay of the Higgs particle $\tilde{h}$ is also allowed from the view point of the generation of baryon number asymmetry.

The condition (26) imposed by the neutrino oscillation data requires $|\lambda_5| = O(10^{-4})$ for the above numerical

---

[6] For a more precise estimation, one could refer to the study in [46], which includes the analysis not only for the phenomenon of mixing of heavy neutrinos, but also for oscillations among the heavy neutrinos.

results. As we will see in the next section, it is consistent with the constraint derived from the dark matter direct search. The values of λ_5 and $\tilde{h}_{\alpha 1}$ used in the above study are found to be realized through Eq. (2) for the cut-off scale such as $M_* = O(10^4)$ TeV, since we assume $\langle S \rangle = M_1$ here. Even if we do not assume this relation and $\langle S \rangle$ is supposed to have a larger value, a similar result is expected to be obtained for a larger value of M_* and smaller values of $|y_i|$ and $|\tilde{y}_i|$.

3 Physics in dark sector

3.1 Relic abundance and detection of dark matter

It is well known that there are three possible mass ranges for an inert doublet dark matter to realize the required relic abundance [47–55]. We are considering the high mass possibility here.[7] The η_R relic abundance can be estimated along the same lines as the original model [31,32,55]. However, we have to take into account that the thermally averaged (co)annihilation cross section $\langle \sigma_{\text{eff}} v \rangle$ has additional contributions from the processes which have X_μ or $\tilde{\sigma}$ in the final states or intermediate states in the present model. Moreover, for the inert doublet dark matter η_R, the direct search imposes severe constraints on the scalar couplings λ_i.

First, we consider the constraint induced through inelastic scattering of η_R with a nucleus. Since the masses of η_R and η_I are almost degenerate for the small values of $|\lambda_5|$ as found from Eq. (6), this inelastic scattering of η_R mediated by the Z^0 exchange brings about substantial effects to the direct search experiments [62–65]. The interaction of η_R relevant to this process is given by

$$\mathcal{L} = \frac{g}{2\cos\theta_W} Z^\mu \left(\eta_R \partial_\mu \eta_I - \eta_I \partial_\mu \eta_R \right). \quad (32)$$

Inelastic η_R-nucleus scattering can occur for η_R whose velocity is larger than the minimum value [66] given by

$$v_{\min} = \frac{1}{\sqrt{2 m_N E_R}} \left(\frac{m_N E_R}{\mu_N} + \delta \right), \quad (33)$$

where δ is the mass difference between η_R and η_I defined in Eq. (6). E_R is the nucleus recoil energy. The mass of the target nucleus and the reduced mass of the nucleus-η_R system are represented by m_N and μ_N. The mass difference δ is constrained by the fact that no dark matter signal has been found in the direct search yet [67–71]. This condition might

---

[7] We note that a much more severe mass degeneracy between the right-handed neutrinos is required in the low mass possibility if the resonant leptogenesis is applied to the model. This is because the wash-out of the generated lepton asymmetry is kept in the thermal equilibrium until a much later period in this case.

be estimated as $\delta \gtrsim 150$ keV [64,65]. Since δ is related to λ_5 through Eq. (6), the condition on δ constrains the value of $|\lambda_5|$ to satisfy [31,32]

$$|\lambda_5| \simeq \frac{M_{\eta_R}\delta}{\langle\phi\rangle^2} \gtrsim 5.0 \times 10^{-6} \left(\frac{M_{\eta_R}}{1 \text{ TeV}} \right) \left(\frac{\delta}{150 \text{ keV}} \right). \quad (34)$$

Since $\tilde{\lambda}_5 = O(1)$ is expected, Eq. (2) suggests that $\langle S \rangle \gtrsim 5 \times 10^{-6} M_*$ should be satisfied.

The present results from a dark matter direct search also impose a constraint on the values of the scalar couplings $\lambda_{3,4}$ and λ_6. The η_R–nucleus elastic scattering is induced through the exchange of $\tilde{h}$ and $\tilde{\sigma}$. The corresponding cross section for η_R–nucleon scattering at zero momentum transfer can be calculated to be

$$\sigma_n^0 = \frac{f^{(n)2} m_n^4 \lambda_+^2}{8\pi M_{\eta_R}^2 m_{\tilde{h}}^4} \left(1 + \frac{\lambda_6^2}{4\kappa\lambda_1} \right)^2, \quad (35)$$

where m_n is a nucleon mass and $f^{(n)} \simeq 0.3$. The second term in the parentheses comes from the $\tilde{\sigma}$ exchange. If we apply the present direct search constraint $\sigma_n^0 < 1 \times 10^{-44}$ cm^2 for $M_{\eta_R} = O(1)$ TeV [69], we find that the scalar couplings $\lambda_{3,4}$ should satisfy

$$\lambda_+ \left(1 + \frac{\lambda_6^2}{4\kappa\lambda_1} \right) < 1.5 \left(\frac{M_{\eta_R}}{1 \text{ TeV}} \right), \quad (36)$$

where $\lambda_+ \simeq \lambda_3 + \lambda_4$. Since the potential stability requires $\lambda_6^2 < 4\kappa\lambda_1$ as seen before, the $\tilde{\sigma}$ exchange contribution to the η_R–nucleon scattering can be generally neglected except for the case where λ_6^2 takes the same value as regards the order, $4\kappa\lambda_1$.

We now proceed to the estimation of the η_R relic abundance taking account of the conditions discussed above. We use the notation $(\eta_1, \eta_2, \eta_3, \eta_4) = (\eta_R, \eta_I, \eta_+, \eta_-)$ for convenience here. The dominant parts of the effective (co)annihilation cross section including the new contributions are calculated to be

$$
\begin{aligned}
\langle \sigma_{\text{eff}} v \rangle \\
\simeq \ & \frac{1}{128\pi M_{\eta_1}^2} \left(\frac{g_2^4(1 + 2\cos^4\theta_W)}{\cos^4\theta_W} + \frac{2g_2^2 g_X^2}{\cos^2\theta_W} + g_X^4 \right) \\
& \times (N_{11} + N_{22} + 2N_{34}) \\
& + \frac{1}{32\pi M_{\eta_1}^2} \left(\frac{g_2^4 \sin^2\theta_W}{\cos^2\theta_W} + g_2^2 g_X^2 \right) (N_{13} + N_{14} + N_{23} + N_{24}) \\
& + \frac{1}{64\pi M_{\eta_1}^2} [\{\lambda_+^2 + \lambda_-^2 + 2(\lambda_3^2 + \lambda_7^2)\}(N_{11} + N_{22}) \\
& + (\lambda_+ - \lambda_-)^2 (N_{33} + N_{44} + N_{12}) + \{(\lambda_+ + \lambda_-)^2 + 4\lambda_3^2 + 2\lambda_7^2\}N_{34} \\
& + \{(\lambda_+ - \lambda_3)^2 + (\lambda_- - \lambda_3)^2\}(N_{13} + N_{14} + N_{23} + N_{24})], \quad (37)
\end{aligned}
$$
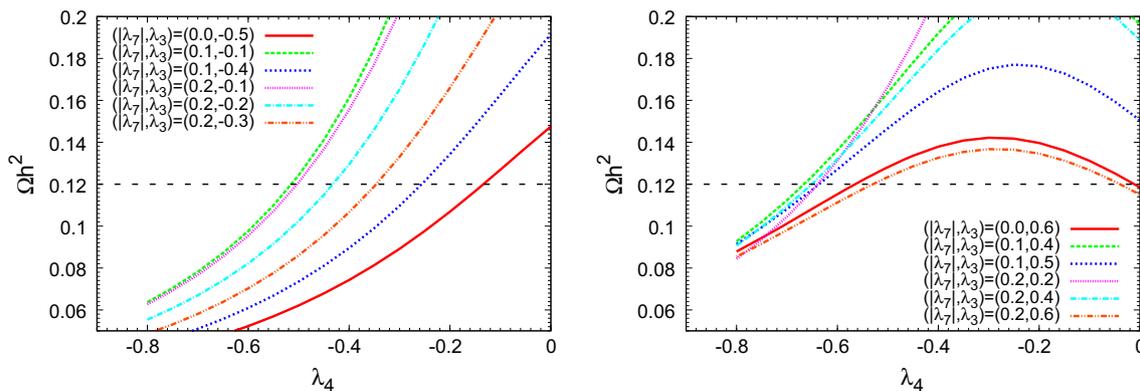
Fig. 3 Relic abundance of η_R in the case of the existence of new interactions. It is plotted as a function of λ_4 for typical sets of $(|\lambda_7|, \lambda_3)$. In the *left* and *right panels*, λ_3 is assumed to be negative and positive, respectively. A *horizontal dashed line* stands for the observed value $\Omega_{\eta_R} h^2 = 0.12$ [13,14]. In this plot, $g_X = 0.1 g_Y$ and $\lambda_5 = -10^{-4}$ are assumed

where g_X is assumed to be much smaller than g_Y and then X_μ is sufficiently lighter than the dark matter η_R. N_{ij} is defined by using $g_{\text{eff}} = \sum_i \frac{n_i^{\text{eq}}}{n_1^{\text{eq}}}$,

$$N_{ij} \equiv \frac{1}{g_{\text{eff}}^2} \frac{n_i^{\text{eq}}}{n_1^{\text{eq}}} \frac{n_j^{\text{eq}}}{n_1^{\text{eq}}} = \frac{1}{g_{\text{eff}}^2} \left(\frac{M_{\eta_i} M_{\eta_j}}{M_{\eta_1}^2} \right)^{\frac{3}{2}}$$
$$\times \exp\left[-\frac{M_{\eta_i} + M_{\eta_j} - 2M_{\eta_1}}{T} \right], \tag{38}$$

where n_i is the η_i number density and n_i^{eq} is its equilibrium value. In order to estimate the relic abundance of η_R, we use the well-known analytic formula instead of solving the Boltzmann equation numerically. The formula is given by [72,73]

$$\Omega_{\eta_1} h^2 \simeq \frac{1.07 \times 10^9 \text{ GeV}^{-1}}{J(x_F) g_*^{\frac{1}{2}} m_{\text{pl}}}, \tag{39}$$

where g_* is for the relativistic degrees of freedom. The freeze-out temperature $T_F (\equiv \frac{M_{\eta_1}}{x_F})$ and $J(x_F)$ are defined as

$$x_F = \ln \frac{0.038 \, m_{\text{pl}} \, g_{\text{eff}} \, M_{\eta_1} \langle \sigma_{\text{eff}} v \rangle}{(g_* x_F)^{\frac{1}{2}}},$$
$$J(x_F) = \int_{x_F}^{\infty} \frac{\langle \sigma_{\text{eff}} v \rangle}{x^2} dx. \tag{40}$$

In Fig. 3 we show the predicted relic abundance of η_R when the new interactions are taken into account. It is plotted as a function of λ_4 by assuming typical values of $(|\lambda_7|, \lambda_3)$. To plot this figure, we assume a small value for g_X, such as $0.1 g_Y$, and we fix the value of $m_\eta^2 + \lambda_7 \langle S \rangle^2$ at 1 TeV^2 for $\langle S \rangle = 2$ TeV. Thus, the mass of X_μ is comparable to the one of the weak bosons and λ_7 is confined to $|\lambda_7| < 0.25$. The figure shows that the above cross section can explain the required dark matter relic abundance for a wide range

of values of $\lambda_{3,4}$. Since the additional (co)annihilation decay processes can generate substantial contributions for a larger $|\lambda_7|$ in this extended model, $|\lambda_3|$ and $|\lambda_4|$ could take much smaller values in comparison with the values required in the original model [31,32]. From the view point of dark matter search, however, the small $|\lambda_7|$ may be promising as suggested through Eq. (35). Since larger values of $|\lambda_{3,4}|$ are required by the relic abundance in this case, the η_R dark matter could be found in the Xenon1T direct search as discussed in [31,32]. On the other hand, it might be difficult to detect even in the Xenon1T experiment in the case of a large $|\lambda_7|$.

3.2 Cosmological signal

In this model, the main phenomenological difference from the original Ma model is the existence of the neutral scalar $\tilde{\sigma}$ and the neutral gauge boson X_μ.[8] They have no direct interaction with the contents of the standard model except for the one caused by the $\lambda_6 S^\dagger S \phi^\dagger \phi$ term. If $\tilde{\sigma}$ is light enough, it induces the Higgs invisible decay through this term as discussed already. Even in that case, if λ_6 satisfies the required condition, the model is consistent with the present data obtained from collider experiments. Moreover, we find no substantial constraint on the masses of $\tilde{\sigma}$ and X_μ from the study of the baryon number asymmetry in the previous section at least for the assumed value of $\langle S \rangle$. On the other hand, these new particles could bring about some crucial influence to the thermal history of the Universe depending on their masses.

First of all, we consider the case where X_μ is heavier than $\tilde{\sigma}$ and then $g_X^2 > 2\kappa$ is satisfied. The new gauge boson X_μ couples only with $\tilde{\sigma}$, η, N_i, and $\tilde{N}_i$. Since the latter three are considered to be much heavier than X_μ, X_μ can decay only to $\gamma \tilde{\sigma}$ and $\ell_\alpha \bar{\ell}_\beta$ through one-loop diagrams with η or N_i and $\tilde{N}_i$ in the internal lines. If we take into account that the neutrino

---

[8] A $U(1)$ extended model has been discussed in a different context [74].

Yukawa couplings $h_{\alpha i}$ and $\tilde{h}_{\alpha i}$ should be of $O(10^{-4})$, we find that the dominant contribution to the X_μ decay comes from the $X_\mu \to \gamma \tilde{\sigma}$ process. Its decay width can be estimated as

$$\Gamma_X \simeq \frac{\alpha_{\text{em}} \mathcal{F}^2}{288(4\pi)^4} \frac{m_X^5}{M_{\eta_c}^4} \left(1 - \frac{M_{\tilde{\sigma}}^2}{m_X^2} \right)^3, \tag{41}$$

where $\mathcal{F} = \lambda_7 - \frac{\lambda_3 \lambda_6}{2\lambda_1}$. If we impose the requirement that $\Gamma_X \gtrsim H$ is satisfied at the temperature where both the freeze-out of the neutron-to-proton ratio and the neutrino decoupling are completed, $\mathcal{F}$ is found to have a lower bound,

$$|\mathcal{F}| \gtrsim 10^{-8} \left(\frac{M_{\eta_c}}{1\,\text{TeV}} \right)^2 \left(\frac{300\,\text{GeV}}{m_X} \right)^{\frac{5}{2}}$$
$$\times \left(\frac{T}{1\,\text{MeV}} \right) \left(1 - \frac{M_{\tilde{\sigma}}^2}{m_X^2} \right)^{-\frac{3}{2}}. \tag{42}$$

Using the constraint on $\lambda_{1,6}$ obtained from the Higgs sector phenomenology and the constraint on $\lambda_{3,7}$ required by the dark matter abundance, $|\mathcal{F}|$ is found to take a large value of $O(0.1)$. This suggests that $\Gamma_X > H$ could be satisfied at the period where the photon temperature is about 1 MeV even for $m_X \gtrsim O(1)$ GeV.

Although the decay product $\tilde{\sigma}$ does not have direct interactions with the standard model contents, it can decay to them through loop effects. Such decay products could affect the cosmological thermal history depending on the time when $\Gamma_{\tilde{\sigma}} \simeq H$ is realized. Since the neutrino Yukawa couplings should be of $O(10^{-4})$, the $\tilde{\sigma}$ decay is dominated by a two photon final state. It is induced through the one-loop diagram with a charged η in the internal line and the decay width can be estimated as

$$\Gamma_{\tilde{\sigma}} \simeq \frac{\alpha_{\text{em}}^2 \mathcal{F}^2}{9216\pi^3 g_X^2} \frac{M_{\tilde{\sigma}}^3 m_X^2}{M_{\eta_c}^4}. \tag{43}$$

If $g_X < 0.88 \kappa^{\frac{3}{10}}$ is satisfied for $g_X^2 > 2\kappa$, $\Gamma_{\tilde{\sigma}}$ is larger than Γ_X. In such a case, $\tilde{\sigma}$ is expected to decay instantaneously after the X_μ decay yields it. Since Eq. (42) shows that this $\tilde{\sigma}$ decay occurs at $T > 1$ MeV, no cosmological effect is expected.

In the other case, $g_X > 0.88 \kappa^{\frac{3}{10}}$, the decay of $\tilde{\sigma}$ occurs with a delay from its production time. If we use the condition $\Gamma_{\tilde{\sigma}} \sim H$ to make a rough estimation of the temperature where the $\tilde{\sigma}$ decay comes in the thermal equilibrium, we have

$$T \sim 54 g_*^{-1/4} \left(\frac{|\mathcal{F}|}{10^{-7}} \right) \left(\frac{1\,\text{TeV}}{M_{\eta_c}} \right)^2 \left(\frac{m_X}{300\,\text{GeV}} \right)^{\frac{3}{2}}$$
$$\times \left(\frac{M_{\tilde{\sigma}}}{m_X} \right)^{\frac{3}{2}} \left(\frac{\langle S \rangle}{2\,\text{TeV}} \right) \text{MeV}. \tag{44}$$

From this result, we find that the $\tilde{\sigma}$ decay could occur before the neutrino decoupling as long as both $|\mathcal{F}|$ and m_X take suitable values for a supposed $M_{\tilde{\sigma}}$. In this case, this decay process does not affect the neutrino effective number in the Universe. For example, the light X_μ such as $m_X = O(1)$ GeV does not affect it for $|\mathcal{F}| > O(10^{-4})$ as long as $10^{-4} m_X < M_{\tilde{\sigma}} < m_X$ is satisfied.

On the other hand, $\ell_\alpha \bar{\ell}_\beta$ could also be a dominant decay mode of X_μ for smaller values of $|\mathcal{F}|$ such as $|\mathcal{F}| \lesssim 10^{-7} \frac{g_X}{g_Y} \left(\frac{\bar{h}}{10^{-4}} \right)^2$. Here, we recall that the averaged value $\bar{h}$ of the relevant neutrino Yukawa couplings $h_{\alpha i}$ is required to be of $O(10^{-4})$ to explain both the neutrino oscillation data and the baryon number asymmetry in the Universe. Such small values of $|\mathcal{F}|$ could be also consistent with the dark matter abundance as long as λ_3 or λ_4 is of $O(1)$ and both $|\lambda_6|$ and $|\lambda_7|$ are small enough. In such a case, this decay process could be in thermal equilibrium still after the neutrino decoupling. The neutrinos produced here could contribute to the effective neutrino number as the non-thermal neutrino components. Although this possibility may be interesting from a cosmological view point, a detailed analysis is beyond the scope of this paper.

Finally, we study the case where X_μ is extremely light and then $\tilde{\sigma}$ is heavier than X_μ. In such a case, the X_μ decay could cause a cosmological problem generally since its decay mode is limited. The cosmological indication could largely change without affecting other results of the model obtained in the previous part. As an interesting example, we address the situation $m_X < 2m_e$ where the gauge coupling g_X becomes unnaturally small.[9] There, X_μ can decay only to neutrino–antineutrino pairs through one-loop diagrams. These non-thermally produced neutrinos affect the present effective neutrino number. Its deviation from the standard value $N_{\text{eff}} = 3.046$ may be estimated [75].

The non-thermal neutrinos make the effective neutrino number shift from the standard value by

$$\Delta N_{\text{eff}}(T) = \frac{120}{7\pi^2} \left(\frac{11}{4} \right)^{\frac{4}{3}} \frac{\rho_\nu^{\text{nth}}(T)}{T^4}, \tag{45}$$

where $\rho_\nu^{\text{nth}}(T)$ is the energy density of non-thermally produced neutrinos at the photon temperature T. This energy density in the co-moving volume R^3 evolves following the differential equation

$$\frac{\text{d}(\rho_\nu^{\text{nth}} R^3)}{\text{d}t} = \Gamma_X(\rho_X R^3) - H(\rho_\nu^{\text{nth}} R^3). \tag{46}$$

---

[9] We note that leptogenesis could occur successfully in this case as found in the third low of Table 2.

Assuming radiation domination through this evolution, we can find the solution

$$\rho_\nu^{\text{nth}} R^3 = m_X N_X^f \frac{1}{\sqrt{\Gamma_X t}} \xi(t), \tag{47}$$

where $\xi(t)$ is defined as $\xi(t) = \text{erf}(\sqrt{\Gamma_X t}) - \sqrt{\Gamma_X t}\, e^{-\Gamma_X t}$ and it is reduced to $\frac{\sqrt{\pi}}{2}$ in the limit $\Gamma_X t \gg 1$. N_X^f stands for the X_μ number in the co-moving volume R^3 at the freeze-out time of X_μ. Since it could be identified with the freeze-out time of η_R, X_μ is relativistic there and then $\frac{N_X^f}{R^3} = \frac{\zeta(3)}{\pi^2} \text{g}_X T^3$ is satisfied. Using these, we finally obtain the deviation of the effective neutrino number due to the non-thermally produced neutrinos:

$$\Delta N_{\text{eff}} = \frac{60\sqrt{2}\zeta(3)}{7\pi^{\frac{7}{2}}} \left(\frac{11}{4}\right)^{\frac{4}{3}} \left(\frac{8\pi^3}{90}\right)^{\frac{1}{4}} \text{g}_R^{\frac{1}{4}} \text{g}_X m_X \sqrt{\frac{1}{\Gamma_X m_{\text{pl}}}}$$

$$\simeq 0.39 \text{g}_X \left(\frac{m_X}{\text{MeV}}\right) \left(\frac{10^{-20}\text{MeV}}{\Gamma_X}\right)^{\frac{1}{2}}, \tag{48}$$

where g_R is for the present degrees of freedom of radiation and it can be approximated by the value of the standard model. This result suggests that the decay width of X_μ should be $\Gamma_X \gtrsim 10^{-20}$ MeV for $X_\mu \to \nu_\alpha \bar{\nu}_\beta$ or $X_\mu \to \nu_\alpha \nu_\beta$ in order to satisfy the present observational results [13,14]. However, since the dominant contribution comes from the latter one, which is induced through a one-loop diagram with the small neutrino Yukawa couplings of $O(10^{-4})$ and also λ_5 of $O(10^{-4})$, the decay width is much smaller than the required value. It means that the neutrinos produced non-thermally through the decay of X_μ give a too large contribution to ΔN_{eff}. Thus, the model with $m_X < 2m_e$ seems to be ruled out by the observed effective neutrino number. If we introduce the kinetic term mixing for X_μ and B_μ, this problem might be evaded even in such a case. This point is briefly discussed in the appendix.

In the present model, the new $U(1)_X$ symmetry is assumed to be local. Even if this symmetry is supposed to be global, the scenario works well in the same way. However, the reasoning for the pairwise introduction of N_i and $\tilde{N}_i$ is lost in the global $U(1)$ case. The difference between them is whether the massless Nambu–Goldstone boson appears after the breaking of $U(1)_X$ symmetry or not. This boson behaves as dark radiation and changes the effective neutrino number in the Universe just in the same way as discussed in [59].

4 Conclusion

We have considered an extension of the radiative neutrino mass model proposed by Ma with a low energy $U(1)$ gauge symmetry. If we assume a cut-off scale of the model at $O(10^4)$ TeV and the breaking of this $U(1)$ at a rather low

energy scale such as $O(1)$ TeV, several assumptions adopted in the original model to explain the neutrino masses, the dark matter abundance, and the baryon number asymmetry in the Universe could be closely related.

We have shown that the breaking of this $U(1)$ symmetry could give a common background for these assumptions. Both the mass degeneracy among the right-handed neutrinos required for the resonant decay of the lightest right-handed neutrino and its small neutrino Yukawa coupling required for the out-of-equilibrium decay could be explained by the same reasoning through this extension. The Z_2 symmetry, which forbids the tree-level neutrino mass generation and guarantees the dark matter stability, has the same origin as the smallness of the quartic coupling constant between the Higgs doublet scalar and the inert doublet scalar, which is an important feature of the model to explain the small neutrino masses. It is useful to recall that these are independent assumptions in the original Ma model. We have also discussed some cosmological issues of the model which appear to be related to this extension. The effective neutrino number could be an interesting subject in this model.

It is interesting that we can have an economical model which could explain the three big problems in the standard model through a simple extension of the Ma model with a low energy $U(1)$ symmetry. A detailed study of the model might give us a clue to the construction of a complete framework beyond the standard model. We will present further results obtained from a quantitative analysis of the related problems in the model elsewhere.

Appendix

In this appendix, we consider cosmological issues in the case with a very light X_μ, where the resonant leptogenesis occurs successfully as discussed in the text. In order to avoid the late time decay of X_μ, we might introduce kinetic term mixing between the gauge fields $\hat{B}_\mu$ and $\hat{X}_\mu$ for the gauge groups $U(1)_Y$ and $U(1)_X$.[10] The kinetic term mixing between them

---

[10] Kinetic term mixing of Abelian gauge fields has been discussed in various phenomenological studies [76–82]. Recent work related to dark matter can be found in [83–90].

may be given by

$$-\frac{1}{4}\hat{F}_{\mu\nu}\hat{F}^{\mu\nu} - \frac{1}{4}\hat{G}_{\mu\nu}\hat{G}^{\mu\nu} - \frac{\sin\chi}{2}\hat{F}_{\mu\nu}\hat{G}^{\mu\nu}, \tag{49}$$

where $\hat{F}_{\mu\nu}$ and $\hat{G}_{\mu\nu}$ are the field strengths of $\hat{B}_\mu$ and $\hat{X}_\mu$, respectively. We can diagonalize these terms by taking the canonically normalized basis B_μ and X_μ as

$$\begin{pmatrix} \hat{B}_\mu \\ \hat{X}_\mu \end{pmatrix} = \begin{pmatrix} 1 & -\tan\chi \\ 0 & \frac{1}{\cos\chi} \end{pmatrix} \begin{pmatrix} B_\mu \\ X_\mu \end{pmatrix}. \tag{50}$$

The modified $U(1)_X$ charge with this new basis is given by

$$Q_X = \frac{\hat{Q}_X}{\cos\chi} + \frac{g_Y}{g_X} Y \tan\chi, \tag{51}$$

where the $U(1)_Y$ charge and both the coupling constants g_Y and g_X are defined as the ones in the no mixing case. This suggests that the standard model contents with $Y \neq 0$ could couple with X_μ as long as the kinetic term mixing exists. As a result, the analysis of the direct search and the relic abundance of dark matter should be modified. In this case, the following new interaction should be added to Eq. (32):

$$\frac{g_X}{2}\left(\frac{1}{\cos\chi} + \frac{g_Y}{2g_X}\right) X^\mu \left(\eta_R \partial_\mu \eta_I - \eta_I \partial_\mu \eta_R\right). \tag{52}$$

If the kinetic term mixing exists, inelastic scattering of η_R can also be brought about by the X_μ exchange. Since both η_R–nucleon scattering cross sections $\sigma_n^0(X_\mu)$ and $\sigma_n^0(Z_\mu)$, which are mediated by the X_μ and Z_μ exchange at zero momentum transfer, can be related each other as

$$\sigma_n^0(X_\mu) \simeq \left(\frac{m_Z^2}{m_X^2}\tan\chi\right)^2 \sigma_n^0(Z_\mu), \tag{53}$$

the present experimental results require that the kinetic term mixing should satisfy

$$\tan\chi \lesssim \frac{m_X^2}{m_Z^2}. \tag{54}$$

This shows that the kinetic term mixing should be sufficiently small for $m_X \lesssim O(1)$ GeV. New non-negligible (co)annihilation modes of η_R to the standard model contents could also appear, depending on the magnitude of the kinetic term mixing $\sin\chi$. However, the constraint (54) suggests that the η_R relic abundance could not be affected by the process mediated through the X_μ exchange. In the study of the η_R relic abundance, even if we introduce the kinetic term mixing, we can neglect the effect of it as long as the condition

(54) is satisfied. Thus, the results obtained in this paper do not change.

As another interesting phenomenon caused by the kinetic term mixing, we consider the X_μ direct decay to the lighter fermions in the standard model through tree diagrams. Its decay width could be estimated as

$$\Gamma_X(f\bar{f}) = \sum_f \frac{g_Y^2}{16\pi m_X}\left(\frac{Y_f}{2}\right)^2 \tan^2\chi. \tag{55}$$

If we impose that $\Gamma_X \gtrsim H$ is satisfied before the neutrino decoupling, we find that the kinetic term mixing should satisfy

$$\tan\chi \gtrsim 10^{-11}\left(\frac{1\text{ GeV}}{m_X}\right)^{\frac{1}{2}}\left(\frac{T}{1\text{ MeV}}\right). \tag{56}$$

This shows that a sufficiently small kinetic term mixing is enough to bring about the X_μ decay to the standard model fermions before the neutrino decoupling. As long as the very small kinetic term mixing exists, the model can overcome the cosmological difficulty for the effective neutrino number in both cases with $m_X > M_{\tilde{\sigma}}$ and $m_X < M_{\tilde{\sigma}}$. Especially, if the kinetic term mixing takes a suitable value in the case $m_X < 1$ MeV, the deviation of the effective neutrino number $N_{\text{eff}} = 3.62 \pm 0.25$, which is suggested through the combined analysis of the data from Planck and the H_0 measurement from the Hubble Space Telescope [13,14], might be explained.

References

1. ATLAS Collaboration, G.Aad et al., Phys. Lett. B **716**, 1 (2012)
2. CMS Collaboration, S.Chatrchyan et al., Phys. Lett. B **716**, 30 (2012)
3. Super-Kamiokande Collaboration, Y. Fukuda et al., Phys. Rev. Lett. **81**, 1562 (1998)
4. SNO Collaboration, Q.R. Ahmad et al., Phys. Rev. Lett. **89**, 011301 (2002)
5. KamLAND Collaboration, K. Eguchi et al., Phys. Rev. Lett. **90**, 021802 (2003)
6. K2K Collaboration, M.H. Ahn et al., Phys. Rev. Lett. **90**, 041801 (2003)
7. T2K Collaboration, K. Abe et al., Phys. Rev. Lett. **107**, 041801 (2011)
8. Double Chooz Collaboration, Y. Abe et al., Phys. Rev. Lett. **108**, 131801 (2012)
9. RENO Collaboration, J.K. Ahn et al., Phys. Rev. Lett. **108**, 191802 (2012)
10. The Daya Bay Collaboration, F.E. An et al., Phys. Rev. Lett. **108**, 171803 (2012)
11. WMAP Collaboration, D.N. Spergel et al., Astrophys. J. Suppl. **148**, 175 (2003)
12. SDSS Collaboration, M. Tegmark et al., Phys. Rev. D **69**, 103501 (2004)
13. Planck Collaboration, P.A.R. Ade et al., Astron. Astrophys. **571**, A16 (2014)

14. Planck Collaboration, P.A.R. Ade et al. arXiv:1502.01589 [astro-ph.CO]
15. A. Riotto, M. Trodden, Ann. Rev. Nucl. Part. Sci. **49**, 35 (1999)
16. W. Bernreuther, Lect. Notes Phys. **591**, 237 (2002)
17. M. Dine, A. Kusenko, Rev. Mod. Phys. **76**, 1 (2003)
18. E. Ma, Phys. Rev. D **73**, 077301 (2006)
19. J. Kubo, E. Ma, D. Suematsu, Phys. Lett. B **642**, 18 (2006)
20. D. Aristizabal Sierra, J. Kubo, D. Restrepo, D. Suematsu, O. Zapata, Phys. Rev. D **79**, 013011 (2009)
21. D. Suematsu, T. Toma, T. Yoshida, Phys. Rev. D **79**, 093004 (2009)
22. D. Suematsu, T. Toma, T. Yoshida, Phys. Rev. D **82**, 013012 (2010)
23. J. Kubo, D. Suematsu, Phys. Lett. B **643**, 336 (2006)
24. D. Suematsu, Eur. Phys. J. C **56**, 379 (2008)
25. H. Fukuoka, J. Kubo, D. Suematsu, Phys. Lett. B **678**, 401 (2009)
26. D. Suematsu, T. Toma, Nucl. Phys. B **847**, 567 (2011)
27. H. Fukuoka, D. Suematsu, T. Toma, JCAP **1107**, 001 (2011)
28. H. Higashi, T. Ishima, D. Suematsu, Int. J. Mod. Phys. A **26**, 995 (2011)
29. D. Suematsu, Eur. Phys. J. C **72**, 72 (2012)
30. D. Suematsu, Phys. Rev. D **85**, 073008 (2012)
31. S. Kashiwase, D. Suematsu, Phys. Rev. D **86**, 053001 (2012)
32. S. Kashiwase, D. Suematsu, Eur. Phys. J. C **73**, 2484 (2013)
33. R.H.S. Buhdi, S. Kashiwase, D. Suematsu, Phys. Rev. D **90**, 113013 (2014)
34. R.H.S. Buhdi, S. Kashiwase, D. Suematsu, JCAP **1509**, 039 (2015)
35. S. Kashiwase, D. Suematsu, Phys. Lett. B **749**, 603 (2015)
36. R.H.S. Buhdi, S. Kashiwase, D. Suematsu, Phys. Rev. D **93**, 013022 (2016)
37. M. Flanz, E.A. Paschos, U. Sarkar, Phys. Lett. B **345**, 248 (1995)
38. L. Covi, E. Roulet, F. Vissani, Phys. Lett. B **384**, 169 (1996)
39. E. Akhmedov, M. Frigerio, A. Yu Smirnov, JHEP **0309**, 021 (2003)
40. C.H. Albright, S.M. Barr, Phys. Rev. D **69**, 073010 (2004)
41. A. Pilaftsis, Phys. ReV. D **56**, 5431 (1997)
42. T. Hambye, J. March-Russell, S.W. West, JHEP **0407**, 070 (2004)
43. A. Pilaftsis, T.E.J. Underwood, Phys. Rev. D **72**, 113001 (2005)
44. A. Pilaftsis, T.E.J. Underwood, Nucl. Phys. B **692**, 303 (2004)
45. J. Beringer et al. (Particle Data Group), Phys. Rev. D **86**, 010001 (2012)
46. P.S. Bhupal Dev, P. Millington, A. Pilatfsis, D. Teresi, Nucl. Phys. B **886**, 569 (2014)
47. R. Barbieri, L.J. Hall, V.S. Rychkov, Phys. Rev. D **74**, 015007 (2006)
48. M. Cirelli, N. Fornengo, A. Strumia, Nucl. Phys. B **753**, 178 (2006)
49. L.L. Honorez, E. Nezri, J.F. Oliver, M.H.G. Tytgat, JCAP **0702**, 028 (2007)
50. Q.-H. Cao, E. Ma, G. Rajasekaran, Phys. Rev. D **76**, 095011 (2007)
51. S. Andreas, M.H.G. Tytgat, Q. Swillens, JCAP **0904**, 004 (2009)
52. E. Nezri, M.H.G. Tytgat, G. Vertongen, JCAP **0904**, 014 (2009)
53. L.L. Honorez, C.E. Yaguna, JCAP **1101**, 002 (2011)
54. M. Gustafsson, S. Rydbeck, L.L. Honorez, E. Lundström, Phys. Rev. D **86**, 075019 (2012)
55. T. Hambye, F.-S. Ling, L.L. Honorez, J. Rocher, JHEP **0907**, 090 (2009)
56. S. Nie, M. Sher, Phys. Lett. B **449**, 89 (1999)
57. S. Kanemura, T. Kasai, Y. Okada, Phys. Lett. B **471**, 182 (1999)
58. P.P. Giardino, K. Kannike, I. Masina, M. Raidal, A. Strumia, JHEP **1405**, 046 (2014)
59. S. Weinberg, Phys. Rev. Lett. **110**, 241301 (2013)
60. M.B. Gavela, T. Hambye, D. Hernandez, P. Hernandez, JHEP **0909**, 038 (2009)
61. D.A. Sierra, A. Degee, J.F. Kamenik, JHEP **1207**, 135 (2012)
62. D.T. Smith, N. Weiner, Phys. Rev. D **72**, 063509 (2005)
63. S. Chang, G.D. Kribs, D.T. Smith, N. Weiner, Phys. Rev. D **79**, 043513 (2009)
64. Y. Cui, D.E. Marrissey, D. Poland, L. Randall, JHEP **0905**, 076 (2009)
65. C. Arina, F.-S. Ling, M.H.G. Tytgat, JCAP **0910**, 018 (2009)
66. D. Smith, N. Weiner, Phys. Rev. D **64**, 043502 (2001)
67. CDMS Collaboration, Z. Ahmed et al., Phys. Rev. Lett. **102**, 011301 (2009)
68. XENON100 Collaboration, E. Aprile et al., Phys. Rev. Lett. **105**, 131302 (2010)
69. LUX Collaboration, D.S. Akerib et al., Phys. Rev. Lett. **112**, 091303 (2014)
70. G. Angloher et al., Astropart. Phys. **31**, 270 (2009)
71. V.N. Lebedenko et al., Phys. Rev. D **80**, 052010 (2009)
72. K. Griest, D. Seckel, Phys. Rev. D **43**, 3191 (1991)
73. P. Gondolo, G. Gelmini, Nucl. Phys. B **360**, 145 (1991)
74. E. Ma, I. Picek, B. Radovcic, Phys. Lett. B **726**, 744 (2013)
75. P. Di Bari, S.F. King, A. Merle, Phys. Lett. B **724**, 77 (2013)
76. B. Holdom, Phys. Lett. B **166**, 196 (1986)
77. T. Matsuoka, D. Suematsu, Prog. Theor. Phys. **76**, 901 (1986)
78. K.R. Dienes, C.F. Kolda, J. March-Russell, Nucl. Phys. B **492**, 104 (1997)
79. B. Holdom, Phys. Lett. B **259**, 329 (1991)
80. K.S. Babu, C.F. Kolda, J. March-Russell, Phys. Rev. D **57**, 6788 (1998)
81. D. Suematsu, Phys. Rev. D **59**, 055017 (1999)
82. D. Suematsu, JHEP **0611**, 029 (2006)
83. R. Foot, R.R. Volkas, Phys. Rev. D **52**, 6595 (1995)
84. C. Boehm, P. Fayet, Nucl. Phys. B **683**, 219 (2004)
85. C. Boehm, P. Fayet, J. Silk, Phys. Rev. D **69**, 101302 (2004)
86. M. Pospelov, A. Ritz, M.B. Voloshin, Phys. Lett. B **662**, 53 (2008)
87. J.L. Feng, J. Kumar, Phys. Rev. Lett. **101**, 231301 (2008)
88. D. Hooper, K.M. Zurek, Phys. Rev. D **77**, 087302 (2008)
89. N. Arkani-Hamed, N. Weiner, JHEP **0812**, 104 (2008)
90. N. Arkani-Hamed, D.P. Finkbeiner, T.R. Slatyer, N. Weiner, Phys. Rev. D **79**, 015014 (2009)